Monthly Notices of the ROYAL ASTRONOMICAL SOCIETY

MNRAS **520,** 3688–3695 (2023) https://doi.org/10.1093/mnras/stad317
Advance Access publication 2023 January 30

Restoring cosmological concordance with early dark energy and massive neutrinos?

Alexander Reeves,[1]★ Laura Herold,[2]★ Sunny Vagnozzi,[3,4]★ Blake D. Sherwin[4,5] and Elisa G. M. Ferreira[6,7]

[1]*Institute for Particle Physics and Astrophysics, ETH Zürich, Wolfgang-Pauli-Straße 27, CH-8093 Zürich, Switzerland*
[2]*Max-Planck-Institut für Astrophysik, Karl-Schwarzschild-Straße 1, D-85740 Garching bei München, Germany*
[3]*Department of Physics, University of Trento, Via Sommarive 14, I-38123 Povo (TN), Italy*
[4]*Kavli Institute for Cosmology, University of Cambridge, Madingley Road, Cambridge CB3 0HA, UK*
[5]*Department of Applied Mathematics and Theoretical Physics, University of Cambridge, Wilberforce Road, Cambridge CB3 0WA, UK*
[6]*Kavli IPMU (WPI), UTIAS, The University of Tokyo, 5-1-5 Kashiwanoha, Kashiwa, Chiba 277-8583, Japan*
[7]*Instituto de Física, Universidade de São Paulo, Rua do Matão 1371, Butantã, 05508-090, São Paulo, Brazil*

Accepted 2023 January 26. Received 2023 January 26; in original form 2022 July 15

ABSTRACT

The early dark energy (EDE) solution to the Hubble tension comes at the cost of an increased clustering amplitude that has been argued to worsen the fit to galaxy clustering data. We explore whether freeing the total neutrino mass M_ν, which can suppress small-scale structure growth, improves EDE's fit to galaxy clustering. Using *Planck Cosmic Microwave Background* and BOSS galaxy clustering data, a Bayesian analysis shows that freeing M_ν does not appreciably increase the inferred EDE fraction $f_{\rm EDE}$: we find the 95 per cent C.L. upper limits $f_{\rm EDE} < 0.092$ and $M_\nu < 0.15\,{\rm eV}$. Similarly, in a frequentist profile likelihood setting (where our results support previous findings that prior volume effects are important), we find that the baseline EDE model (with $M_\nu = 0.06\,{\rm eV}$) provides the overall best fit. For instance, compared to baseline EDE, a model with $M_\nu = 0.24\,{\rm eV}$ maintains the same H_0(km/s/Mpc) = (70.08, 70.11, respectively) whilst decreasing $S_8 = (0.837, 0.826)$ to the ΛCDM level, but worsening the fit significantly by $\Delta\chi^2 = 7.5$. For the datasets used, these results are driven not by the clustering amplitude, but by background modifications to the late-time expansion rate due to massive neutrinos, which worsen the fit to measurements of the BAO scale.

Key words: cosmic background radiation – large-scale structure of the universe – dark energy – cosmological parameters – cosmology: observations.

1 INTRODUCTION

The Hubble tension, i.e. the disagreement between independent measurements of the Hubble constant H_0, is arguably among cosmology's main open problems (Di Valentino et al. 2021; Perivolaropoulos & Skara 2022; Abdalla et al. 2022). While systematics cannot be excluded (Freedman et al. 2019; Efstathiou 2020; Mortsell et al. 2022), serious consideration has been given to the possibility of new physics being at the origin of the tension, given its persistence (Mörtsell & Dhawan 2018; Guo, Zhang & Zhang 2019; Vagnozzi 2020). Consistency with Baryon Acoustic Oscillation (BAO) and uncalibrated SNeIa data requires new physics to preferably operate before recombination, in order to reduce the sound horizon by ~ 7 per cent (Bernal, Verde & Riess 2016; Addison et al. 2018; Lemos et al. 2019; Aylor et al. 2019; Knox & Millea 2020).

One scenario invoked in this context is early dark energy (EDE), a model which introduces a pre-recombination dark energy (DE) like component that boosts the expansion rate (reducing the sound horizon) before decaying (Poulin et al. 2019). EDE fares well when confronted with Cosmic Microwave Background (CMB) and low-z background data (see, however, Krishnan et al. 2020), but was argued to be in tension with weak lensing (WL) and large-scale structure (LSS) data (Hill et al. 2020; Ivanov et al. 2020c; D'Amico et al. 2021). It was hinted in Murgia, Abellán & Poulin (2021) and Smith et al. (2021), and shown in Herold, Ferreira & Komatsu (2022) that marginalization effects affect these analyses: a frequentist profile likelihood (PL) analysis found that large EDE fractions $f_{\rm EDE}$ are not ruled out by galaxy clustering data. However, parameter shifts in high $f_{\rm EDE}$ cosmologies lead to an increase in the clustering amplitude σ_8 and the related parameter S_8, worsening the 'S_8 discrepancy' (Di Valentino & Bridle 2018; Nunes & Vagnozzi 2021).

In this work, we study the influence of massive neutrinos on EDE, motivated by their free-streaming nature, whose associated power suppression might counteract the EDE-induced enhancement and provide a better fit to LSS data. We find no clear benefits for EDE resulting from massive neutrinos, neither in a Bayesian nor in a frequentist setting. We investigate prior volume effects, and physical effects driving our parameter constraints, which overall motivate further studies of EDE cosmologies with massive neutrinos.

2 EDE AND MASSIVE NEUTRINOS

The simplest EDE models envisage an ultra-light scalar field initially displaced from the minimum of its potential and frozen by

★ E-mail: areeves@phys.ethz.ch (AR); lherold@mpa-garching.mpg.de (LH); sunny.vagnozzi@unitn.it (SV)

Hubble friction, behaving as a DE component boosting the pre-recombination expansion rate.[1] Once the Hubble rate drops below its effective mass, the field becomes dynamical, rolls down, and oscillates around the minimum of its potential. The canonical EDE model features a pseudoscalar (axion-like) field with the following potential:

$$V(\phi) = m^2 f^2 \left[1 - \cos\left(\frac{\phi}{f}\right)\right]^n , \quad (1)$$

where m and f are the EDE mass and decay constant. With this choice of potential, EDE later decays as a fluid with effective equation of state $\langle w_\phi \rangle = (n-1)/(n+1)$.

The fundamental particle physics parameters m and f can be traded for the phenomenological parameters $f_{\rm EDE}$ and z_c: at redshift z_c, EDE's fractional contribution to the energy density is maximal and equal to $f_{\rm EDE} = \rho_{\rm EDE}/3M_{\rm Pl}^2 H(z_c)^2$, where $\rho_{\rm EDE}$ is EDE's energy density, $M_{\rm Pl}$ is the *Planck* mass, and $H(z)$ is the Hubble rate. The physics of the EDE model is then governed by four parameters: $f_{\rm EDE}$, z_c, n, and the initial misalignment angle $\theta_i = \phi_i/f$, with ϕ_i the initial field value. For simplicity we set $n = 3$, corresponding to the best-fitting value reported by Poulin et al. (2019). Increasing $f_{\rm EDE}$ reduces $r_{\rm drag}$, the sound horizon at the drag epoch, and solving the Hubble tension requires $f_{\rm EDE} \gtrsim 0.1$.

To compensate for the EDE-induced enhancement of the early integrated Sachs–Wolfe (eISW) effect and preserve the fit to the CMB (Vagnozzi 2021), EDE's success comes at the significant cost of an increase in the dark matter (DM) density $\omega_c = \Omega_c h^2$. This boosts the matter power spectrum and raises $S_8 \propto \sigma_8\sqrt{\Omega_m}$, worsening the S_8 discrepancy present within ΛCDM (see Fig. 1). EDE was thus argued to be disfavoured by WL and galaxy clustering data (Hill et al. 2020), although Murgia et al. (2021), Smith et al. (2021), Herold et al. (2022), and Gómez-Valent (2022) argued that this is in part due to prior volume effects (PVEs). [2]

A possible remedy is to add extra components absorbing the excess power (e.g. Allali, Hertzberg & Rompineve 2021; Clark et al. 2021; Ye, Zhang & Piao 2021). Massive neutrinos are an economical and conservative candidate in this sense as we know oscillation experiments show that at least two neutrino mass eigenstates are massive. Including a free neutrino mass sum M_ν (rather than fixing it to the minimum allowed value of 0.06 eV as in baseline EDE) can thus be justified invoking only known physics and this inclusion has not been explored in this context so far. Due to their free-streaming nature, massive neutrinos suppress small-scale power (Lesgourgues & Pastor 2006): Fig. 1 shows how values of $M_\nu \approx 0.3$ eV can in principle absorb the EDE-induced excess power in a wavenumber range relevant to current surveys. Note that models connecting EDE to neutrinos and predicting high M_ν have been studied (Sakstein & Trodden 2020; Carrillo González et al. 2021), alongside the role of neutrino physics in relation to cosmic tensions (Ilić, Sakr & Blanchard 2019; Chudaykin, Gorbunov & Nedelko 2022; Das et al. 2022; Di Valentino & Melchiorri 2022; Sakr, Ilic & Blanchard 2022).

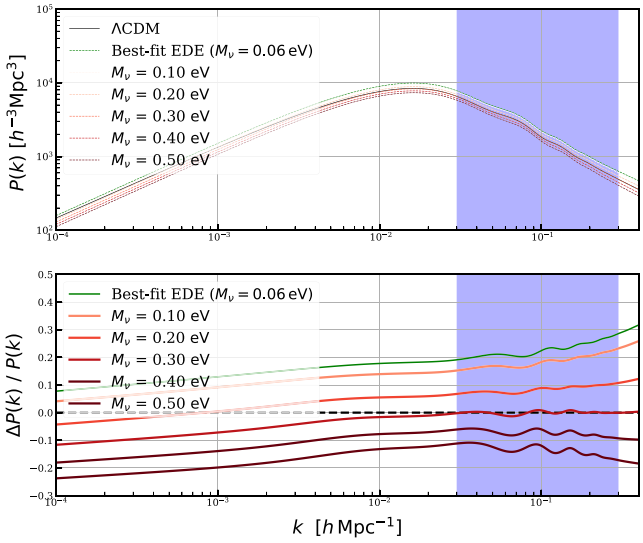

Figure 1. Impact of M_ν on the EDE matter power spectrum, with the other parameters (including θ_s and nuisance parameters) fixed to the best-fitting values of Hill et al. (2020). *Lower panel*: relative change with respect to ΛCDM. The purple region is the wavenumber range of interest to current surveys.

Adding M_ν as a free parameter within ΛCDM induces well-known parameter degeneracies at the CMB level: a negative M_ν-H_0 correlation related to the geometrical degeneracy and a positive M_ν-ω_c correlation connected to the CMB lensing amplitude (Vagnozzi et al. 2018; Roy Choudhury & Hannestad 2020). BAO data partially aid in breaking these degeneracies (especially the M_ν-H_0 one). At fixed acoustic scale θ_s, increasing M_ν reduces the BAO angular scale $\theta_{\rm BAO} = r_{\rm drag}/D_V(z_{\rm eff})$ (Hou et al. 2014; Archidiacono et al. 2017; Boyle & Komatsu 2018), with $D_V(z_{\rm eff})$ the volume-averaged distance at the effective redshift $z_{\rm eff}$.

3 DATASETS AND METHODOLOGY

We use *Planck* 2018 CMB temperature, polarization, and lensing measurements, combining the `Plik TTTEEE`, `lowl`, `lowE`, and `lensing` likelihoods (Aghanim et al. 2020a). We add the joint pre-reconstruction full-shape (FS) plus post-reconstruction BAO likelihood for the BOSS DR12 galaxies (see Ivanov, Simonović & Zaldarriaga 2020a; Philcox et al. 2020).[3] The cross-covariance between FS and BAO is fully taken into account in the likelihood. The FS measurements include both the monopole and quadrupole moments. We do not include a distance ladder H_0 prior to not bias H_0 towards high values (see also Efstathiou 2021).

We consider a 10-parameter EDE + M_ν model, where, besides the 6 ΛCDM parameters, M_ν and 3 EDE parameters ($f_{\rm EDE}$, $\log_{10} z_c$, and θ_i, fixing $n = 3$) are varied. The neutrino mass spectrum is modelled following the degenerate approximation, sufficiently accurate for the

[1]For examples of other EDE(-like) models, see Karwal & Kamionkowski (2016), Agrawal et al. (2019), Alexander & McDonough (2019), Lin et al. (2019), Niedermann & Sloth (2021), Ye & Piao (2020), Zumalacarregui (2020), Gogoi et al. (2021), Ballesteros, Notari & Rompineve (2020), Braglia et al. (2020a), Braglia et al. (2020b), Braglia et al. (2021), Oikonomou (2021), Freese & Winkler (2021), Nojiri et al. (2021), Karwal et al. (2022), Khosravi & Farhang (2022), Niedermann & Sloth (2022), Sabla & Caldwell (2022), and Benevento et al. (2022).

[2]In the above, the CMB data is from *Planck*. Mild preferences for EDE have been found from ACT or SPT data, or dropping *Planck* high-ℓ data (Chudaykin, Gorbunov & Nedelko 2020a; Jiang & Piao 2021; Poulin, Smith & Bartlett 2021; Hill et al. 2022; Jiang & Piao 2022; Jiang, Ye & Piao 2022; La Posta et al. 2022; Ye, Jiang & Piao 2022), but consensus on these results is lacking, due to possible systematics (e.g. Handley & Lemos 2021; Smith et al. 2022).

[3]In future work, we will study the impact of updates in the modelling of the window function (Beutler & McDonald 2021). We do not expect a big impact on our constraints, which are driven by the BAO scale.

precision of current data (Vagnozzi et al. 2017; Giusarma et al. 2018; Archidiacono, Hannestad & Lesgourgues 2020; Roy Choudhury & Hannestad 2020; Tanseri et al. 2022). For comparison, we also consider three related models: 9-parameter EDE ($M_\nu = 0.06\,\mathrm{eV}$), 7-parameter $\Lambda\mathrm{CDM} + M_\nu$ ($f_{\mathrm{EDE}} = 0$), and the standard 6-parameter $\Lambda\mathrm{CDM}$.

Theoretical predictions are computed using the `EDE-CLASS-PT` Boltzmann solver,[4] itself a merger of `CLASS_EDE` (Hill et al. 2020) and `CLASS-PT` (Philcox et al. 2020), themselves both extensions to the Boltzmann solver `CLASS` (Blas, Lesgourgues & Tram 2011). The underlying galaxy power spectrum model is based on the Effective Field Theory of LSS (EFTofLSS, Baumann et al. 2012), which is the most general, symmetry-driven model for the mildly non-linear clustering of biased tracers of the LSS, accounting for the complex and poorly known details of short-scale physics which are integrated out.

We follow two analysis methods. We begin with a standard Bayesian analysis, adopting Monte Carlo Markov Chain (MCMC) methods and using the `MontePython` MCMC sampler (Audren et al. 2013; Brinckmann & Lesgourgues 2019). We impose the same (flat) priors on the EDE parameters as in Hill et al. (2020), whereas for the EFTofLSS nuisance parameters we follow Philcox et al. (2020). We monitor the convergence of the generated MCMC chains via the Gelman–Rubin parameter $R - 1$ (Gelman & Rubin 1992), with the chains considered to be converged if $R - 1 < 0.05$ (which, we note, is a more stringent requirement than that adopted by several other EDE works). Following the conclusions of Herold et al. (2022), Herold & Ferreira (2022), and the analysis in Ade et al. (2014) for varying neutrino mass sum, we then perform a PL analysis in M_ν: for a given (fixed) value of M_ν, after minimizing the χ^2 with respect to all other parameters, the PL is given by $\Delta\chi^2(M_\nu)$. We follow the minimization method of Schöneberg et al. (2022), referred to as S21, running a series of MCMCs with decreased temperature and enhanced sensitivity to likelihood differences. For comparison, we also use the gradient descent-based `MIGRAD` algorithm (James & Roos 1975), finding that S21 always outperforms it for the EDE model.

4 RESULTS

From the *Planck*+BOSS combination, a Bayesian analysis of the EDE + M_ν model returns the 95 per cent confidence level (C.L.) upper limit $M_\nu < 0.151\,\mathrm{eV}$. This is only slightly weaker than the corresponding $\Lambda\mathrm{CDM} + M_\nu$ limit from the same dataset ($M_\nu < 0.147\,\mathrm{eV}$), safely excluding the ballpark region required to compensate the EDE enhancement ($M_\nu \sim 0.3\,\mathrm{eV}$). This reflects in sub-$\sigma$ shifts and slightly broader uncertainties in H_0, σ_8, and f_{EDE}, compared to their baseline EDE ($M_\nu = 0.06\,\mathrm{eV}$) counterparts [in brackets]: $H_0 = 68.71 \pm 1.06\,[68.72 \pm 0.90]\,\mathrm{km/s/Mpc}$, $S_8 = 0.826 \pm 0.012\,[0.826 \pm 0.012]$, $f_{\mathrm{EDE}} < 0.092\,[< 0.085]$, see also Fig. 2. These sub-σ shifts show that, in a Bayesian setting, freeing M_ν does not significantly increase the inferred f_{EDE}, with the peak of the posterior still being close to zero.

We then perform a PL analysis, fixing M_ν to seven values between 0.06 eV and 0.3 eV and dissecting each likelihood's contribution to the total χ^2. We aim to identify *(a)* which dataset(s) prevent high M_ν values and *(b)* whether PVEs are playing a role. Smith, Poulin & Amin (2020), Herold et al. (2022), and Gómez-Valent (2022) argued that PVEs play a key role with EDE, as in the $f_{\mathrm{EDE}} \to 0$ limit $\Lambda\mathrm{CDM}$ is recovered, so the likelihood is approximately flat in the θ_i and z_c directions. This leads to a larger prior volume in the low f_{EDE} region, resulting in a preference for small f_{EDE} upon marginalization. The PL is not impacted by these PVEs.

Our PL analysis results are shown in Figs. 3 and 4. We find that the baseline EDE model ($M_\nu = 0.06\,\mathrm{eV}$) with $f_{\mathrm{EDE}} = 0.077$ fits the data best. This has a $\Delta\chi^2 = -5.6$ compared to the baseline $\Lambda\mathrm{CDM}$ model, although we have introduced three extra parameters (when fixing M_ν). Following Akaike (1974), we can compute the Akaike information criterion (AIC), a measure of statistical preference for models. It accounts for a differing number of free parameters, penalizing a higher number of free parameters, which does not lead to a sufficient improvement in fit. For a given model it is given by:

$$\mathrm{AIC} = 2k + \min(\chi^2) \tag{2}$$

where k is the number of model parameters, and where a lower AIC indicates a model which is statistically preferred. For the EDE model with $M_\nu = 0.06\,\mathrm{eV}$ we find $\Delta\mathrm{AIC} = +0.4$ compared to $\Lambda\mathrm{CDM}$, indicating a mild statistical preference for $\Lambda\mathrm{CDM}$ despite the overall reduction in χ^2. The best-fitting f_{EDE} for this model is significantly higher than the mean value expected from the Bayesian results for the baseline model with $M_\nu = 0.06\,\mathrm{eV}$ (see also the purple star in Fig. 2); hence, we reconfirm the results of Herold et al. (2022) and Gómez-Valent (2022) that PVEs could have an impact on the Bayesian constraints of the baseline EDE model. However, even once this effect is accounted for in the PL analysis, there is no evidence of benefit from a raised M_ν in the EDE scenario. Lowering S_8 to the $\Lambda\mathrm{CDM}$ level within EDE requires $M_\nu \sim 0.24\,\mathrm{eV}$ ($S_8 = 0.826, f_{\mathrm{EDE}} = 0.117$). This comes at the cost of a substantially worse fit quality ($\Delta\chi^2 = 7.5$), clearly disfavouring this model.

The PL in M_ν, broken down into the χ^2 contributions from the individual datasets in our analysis is shown in the blue and purple lines in Fig. 3 (related information is shown in Fig. 4). We find that the fit to both the *Planck* TTTEEE + lensing and the BOSS data worsens as M_ν is increased. For the *Planck* data, the strong constraining power on M_ν is expected (Aghanim et al. (2020b) for $\Lambda\mathrm{CDM}$). More interestingly, the fit to the BOSS dataset also degrades monotonically with M_ν: this suggests that the benefits of increased M_ν in the EDE scenario in terms of a reduction in clustering amplitude are being outweighed by an increasing mismatch to the geometric features of the FS spectrum. We find that most of the effect of EDE-induced parameter shifts and M_ν on the FS clustering amplitude is re-absorbed by nuisance parameter shifts, as pointed out in Ivanov et al. (2020c) within baseline EDE. The remaining differences in the galaxy power spectrum multipoles are due to a mismatch in the location of the BAO wiggles. Hence, the derived constraints on the EDE + M_ν model are mostly driven by shifts in the BAO scale θ_{BAO}, rather than the M_ν-driven small-scale power suppression (see further discussion in Appendix 5). In Fig. 5, we show how the fit to the BAO scale gradually worsens as M_ν increases, reflecting the increasing trend in the BOSS likelihood χ^2.

The increase in M_ν is accompanied by different parameter shifts as demonstrated in Fig. 4. We find a M_ν-f_{EDE} correlation, which can be understood as follows. Increasing M_ν at fixed θ_s and $\omega_b + \omega_c$ results in the $z \lesssim 1$ expansion rate decreasing relative to a $M_\nu = 0$ model (see a complete explanation in Hou et al. 2014; Archidiacono et al. 2017), decreasing θ_{BAO}. In contrast, raising f_{EDE} leads to a fractional decrease in r_{drag}, which, as a result of the accompanying increase in H_0, results in a larger fractional decrease in $D_V(z_{\mathrm{eff}})$. The overall effect is to (re-)increase θ_{BAO}, as we checked numerically. The net result is that θ_{BAO} still decreases when increasing M_ν and f_{EDE} simultaneously, but less so than if we had kept f_{EDE} fixed. The extent to which f_{EDE} can compensate for the M_ν-induced reduction

[4] https://github.com/Michalychforever/EDE_class_pt

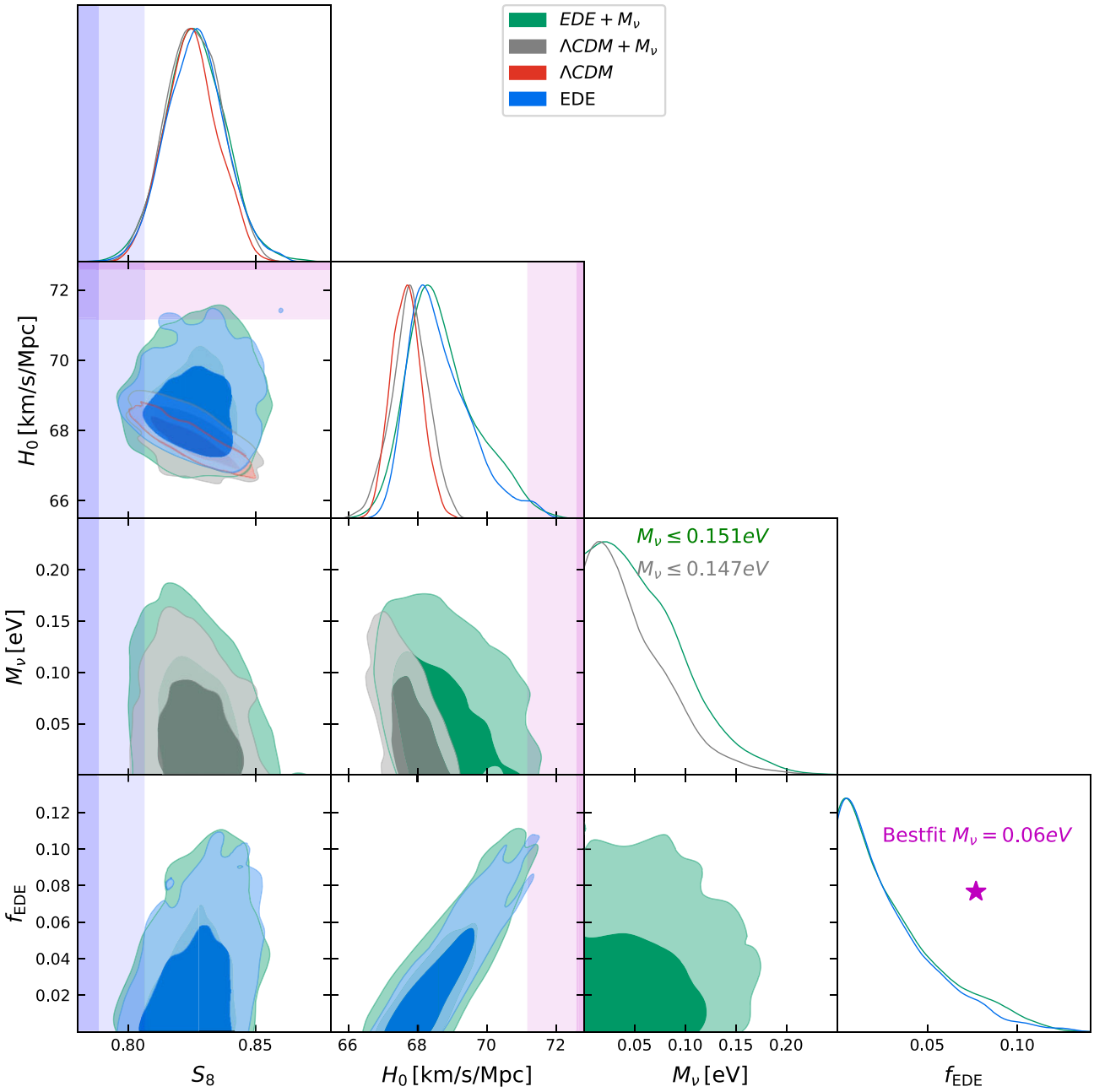

Figure 2. 1D and 2D posteriors for S_8, H_0, $f_{\rm EDE}$, and M_ν within different models (see colour coding). These contours represent the Bayesian constraints obtained when combining *Planck* and BOSS (FS + BAO) data. Pink bands indicate the SH0ES local H_0 measurement from Riess et al. (2022) and purple bands denote the inverse-variance-weighed combination of *DES-Y1+KiDS + HSC* S_8 measurements as in Hill et al. (2020). The best-fitting $f_{\rm EDE}$ value with fixed $M_\nu = 0.06$ eV is shown as a purple star.

of $\theta_{\rm BAO}$ is strongly limited by the accompanying increase in ω_c (compensating the eISW boost), whose effect is similar to that of raising M_ν, overall (re-)decreasing $\theta_{\rm BAO}$. As a result, the best-fitting H_0 barely shifts when M_ν is raised. These arguments easily extend to anisotropic BAO measurements (see also Klypin et al. 2021). See Lattanzi & Gerbino (2018), Vagnozzi (2019), and Sakr (2022) for more complete discussions on the effect of massive neutrinos on various cosmological probes.

For $M_\nu \gtrsim 0.18$ eV, the χ^2 increases more steeply, mostly driven by the BOSS likelihood due to the gradually worsened BAO scale fit. However, H_0 remains stable within 1 per cent across the whole M_ν range, due to two competing effects: while increasing $f_{\rm EDE}$ pulls H_0 upwards, increasing M_ν lowers it due to the geometrical degeneracy. As discussed earlier, increasing M_ν is accompanied by decreases in σ_8 and S_8.

5 CONCLUSIONS

It is well known that introducing EDE in order to resolve the H_0 tension worsens the 'S_8 tension'. Our paper re-examines this issue in light of an extension including massive neutrinos, driven by the possibility of their small-scale power suppression counteracting the EDE-induced excess power, which leads to the increase in S_8.

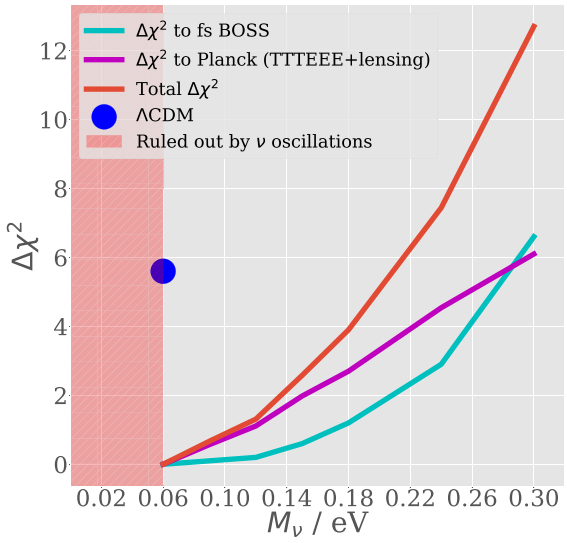

Figure 3. χ^2 contributions as a function of M_ν within the EDE model. The purple and blue lines respectively show the χ^2 contribution from the *Planck* and BOSS likelihoods and the red line is the total χ^2, given by the sum of the two. The blue dot represents the best-fitting ΛCDM model, given the same combination of data. The red-shaded region encompasses values of M_ν which are ruled out by oscillation experiments. The full table of best-fitting results is shown in Appendix A.

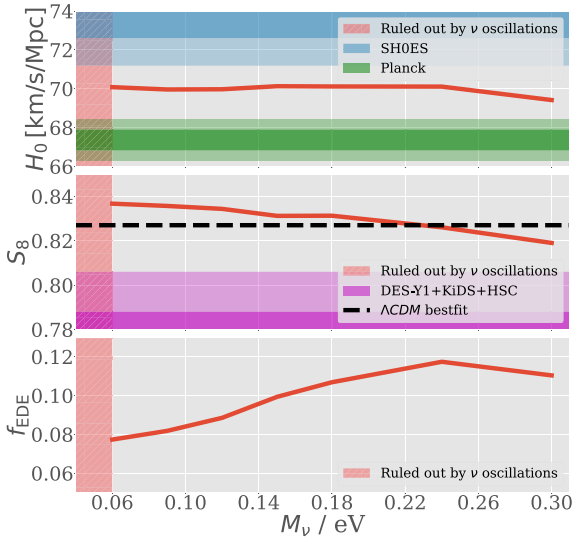

Figure 4. Variation in the best-fitting values of selected cosmological parameters as a function of M_ν. The red-shaded region encompasses values of M_ν that are ruled out by oscillation experiments. The blue and green bands indicate, respectively, the value of H_0 inferred from *Planck* assuming the ΛCDM model (Aghanim et al. 2020b), and the SH0ES local distance ladder value (Riess et al. 2022). The purple band is an inverse-variance-weighed combination of DES-Y1+KiDS + HSC S_8 measurements as in Hill et al. (2020), whilst the black dashed line is the best-fitting value of S_8 from a fit to the same datasets assuming ΛCDM. The full table of best-fitting values is shown in Appendix 5.

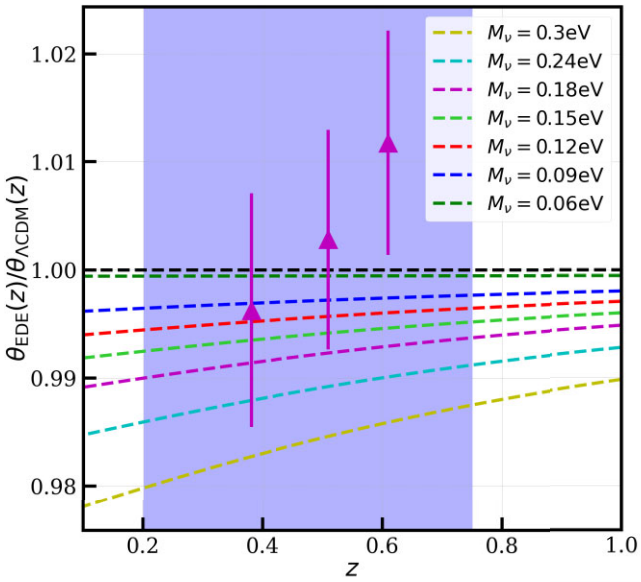

Figure 5. BAO angular scale within EDE at fixed values of M_ν relative to the ΛCDM predictions (all parameters fixed to their *Planck* + BOSS best fits). Purple triangles denote the BOSS DR12 consensus isotropic BAO measurements (Alam et al. 2017).

A standard Bayesian analysis of CMB and galaxy clustering data shows that freeing M_ν does not increase the inferred $f_{\rm EDE}$ and has no effect on EDE's standings relative to the H_0 and S_8 tensions. A frequentist PL analysis also finds no clear benefits for EDE resulting from a higher M_ν, as the best fit is achieved within baseline EDE ($M_\nu = 0.06$ eV), but supports earlier claims of PVEs playing a key role in these Bayesian constraints using BOSS data (Smith et al. 2021; Herold et al. 2022; Gómez-Valent 2022). Values of M_ν lowering S_8 to the ΛCDM level are not preferred statistically; a model with $M_\nu = 0.24$ eV worsens the fit by $\Delta\chi^2 = 7.5$ in comparison to baseline EDE. We find a correlation between $f_{\rm EDE}$ and M_ν, along with the expected negative M_ν-S_8 correlation. [5]

Contrary to initial expectations, our M_ν limits are driven not by the FS clustering amplitude (re-absorbed by nuisance parameters), but by shifts in the BAO scale $\theta_{\rm BAO}$. As the clustering amplitude plays a minor role, our analysis is not very sensitive to the benefits of the M_ν-driven power suppression. One possible avenue for further work would be to explore the inclusion of WL data or WL-derived priors which, without freeing M_ν, appear to slightly decrease the value of $f_{\rm EDE}$ and consequently H_0 (Herold & Ferreira 2022); it will be interesting to study whether freeing M_ν can improve the consistency of EDE with WL measurements. A related recent paper by some of us, which appeared after ours was posted on arXiv, has derived new PL-based confidence intervals on EDE using additional datasets (including a Gaussian likelihood centred on the S_8 of the Dark Energy Survey Year 3 analysis, see Herold & Ferreira 2022).

[5] As a caveat, we note that the perturbation theory and mode-coupling kernels used in `CLASS-PT` have been computed assuming an Einstein-de Sitter Universe, whereas here we are including both EDE and neutrino masses: as these new physics contributions do not violate the equivalence principle, this is a reasonable approximation (although one that would need to be refined for future more precise data), see e.g. more complete recent discussions in Sec. IVF of Chudaykin et al. (2020b) and Sec. IIB of Nunes et al. (2022), with similar considerations holding for the IR resummation procedure.

In the coming years, β-decay experiments will aim for a model-independent kinematical neutrino mass detection, which, combined with future cosmological probes (Ade et al. 2019; Abitbol et al. 2019), will set the stage for further tests of EDE and massive neutrinos.

ACKNOWLEDGEMENTS

We thank George Efstathiou, Colin Hill, Eiichiro Komatsu, and Oliver Philcox for many useful discussions. S.V. was partially supported by the Isaac Newton Trust and the Kavli Foundation through a Newton–Kavli Fellowship and by a grant from the Foundation Blanceflor Boncompagni Ludovisi, née Bildt. B.D.S. is supported by the European Research Council (Grant agreement No. 851274) and an STFC Ernest Rutherford Fellowship. The Kavli IPMU is supported by World Premier International Research Center Initiative (WPI), MEXT, Japan.

DATA AVAILABILITY

The data underlying this article will be shared upon request to the corresponding author(s).

REFERENCES

Abdalla E. et al., 2022, JHEAp, 34, 49
Abitbol M. H. et al., 2019, Bull. Am. Astron. Soc., 51, 147
Addison G. E., Watts D. J., Bennett C. L., Halpern M., Hinshaw G., Weiland J. L., 2018, Astrophys. J., 853, 119
Ade P. A. R. et al., 2014, Astron. Astrophys., 566, A54
Ade P. et al., 2019, JCAP, 02, 056
Aghanim N. et al., 2020a, Astron. Astrophys., 641, A5
Aghanim N. et al., 2020b, Astron. Astrophys., 641, A6
Agrawal P., Cyr-Racine F.-Y., Pinner D., Randall L., 2019, preprint (arXiv:1904.01016)
Akaike H., 1974, IEEE Trans. Autom. Control, 19, 716
Alam S. et al., 2017, MNRAS, 470, 2617
Alexander S., McDonough E., 2019, Phys. Lett. B, 797, 134830
Allali I. J., Hertzberg M. P., Rompineve F., 2021, Phys. Rev. D, 104, L081303
Archidiacono M., Brinckmann T., Lesgourgues J., Poulin V., 2017, JCAP, 02, 052
Archidiacono M., Hannestad S., Lesgourgues J., 2020, JCAP, 09, 021
Audren B., Lesgourgues J., Benabed K., Prunet S., 2013, JCAP, 02, 001
Aylor K., Joy M., Knox L., Millea M., Raghunathan S., Wu W. L. K., 2019, Astrophys. J., 874, 4
Ballesteros G., Notari A., Rompineve F., 2020, JCAP, 11, 024
Baumann D., Nicolis A., Senatore L., Zaldarriaga M., 2012, JCAP, 07, 051
Benevento G., Kable J. A., Addison G. E., Bennett C. L., 2022, Astrophys. J., 935, 156
Bernal J. L., Verde L., Riess A. G., 2016, JCAP, 10, 019
Beutler F., McDonald P., 2021, JCAP, 11, 031
Blas D., Lesgourgues J., Tram T., 2011, JCAP, 07, 034
Boyle A., Komatsu E., 2018, JCAP, 03, 035
Braglia M., Ballardini M., Emond W. T., Finelli F., Gumrukcuoglu A. E., Koyama K., Paoletti D., 2020a, Phys. Rev. D, 102, 023529
Braglia M., Emond W. T., Finelli F., Gumrukcuoglu A. E., Koyama K., 2020b, Phys. Rev. D, 102, 083513
Braglia M., Ballardini M., Finelli F., Koyama K., 2021, Phys. Rev. D, 103, 043528
Brinckmann T., Lesgourgues J., 2019, Phys. Dark Univ., 24, 100260
Carrillo González M., Liang Q., Sakstein J., Trodden M., 2021, JCAP, 04, 063
Chudaykin A., Gorbunov D., Nedelko N., 2020a, JCAP, 08, 013
Chudaykin A., Ivanov M. M., Philcox O. H. E., Simonović M., 2020b, Phys. Rev. D, 102, 063533
Chudaykin A., Gorbunov D., Nedelko N., 2022, preprint (arXiv:2203.03666)
Clark S. J., Vattis K., Fan J., Koushiappas S. M., 2021, preprint (arXiv:2110.09562)
D'Amico G., Senatore L., Zhang P., Zheng H., 2021, JCAP, 05, 072
Das S., Maharana A., Poulin V., Sharma R. K., 2022, Phys. Rev. D, 105, 103503
Di Valentino E., Bridle S., 2018, Symmetry, 10, 585
Di Valentino E., Melchiorri A., 2022, Astrophys. J. Lett., 931, L18
Di Valentino E. et al., 2021, Class. Quantum Gravity, 38, 153001
Efstathiou G., 2020, preprint (arXiv:2007.10716)
Efstathiou G., 2021, MNRAS, 505, 3866
Freedman W. L. et al., 2019, Astrophys. J., 882, 34
Freese K., Winkler M. W., 2021, Phys. Rev. D, 104, 083533
Gelman A., Rubin D. B., 1992, Stat. Sci., 7, 457
Giusarma E., Vagnozzi S., Ho S., Ferraro S., Freese K., Kamen-Rubio R., Luk K.-B., 2018, Phys. Rev. D, 98, 123526
Gogoi A., Sharma R. K., Chanda P., Das S., 2021, Astrophys. J., 915, 132
Gómez-Valent A., 2022, Phys. Rev. D, 106, 063506
Guo R.-Y., Zhang J.-F., Zhang X., 2019, JCAP, 02, 054
Handley W., Lemos P., 2021, Phys. Rev. D, 103, 063529
Herold L., Ferreira E. G. M., Komatsu E., 2022, Astrophys. J. Lett., 929, L16
Herold L., Ferreira E. G. M., 2022, preprint (arXiv:2210.16296)
Hill J. C., McDonough E., Toomey M. W., Alexander S., 2020, Phys. Rev. D, 102, 043507
Hill J. C. et al., 2022, Phys. Rev. D, 105, 123536
Hou Z. et al., 2014, Astrophys. J., 782, 74
Ilić S., Sakr Z., Blanchard A., 2019, Astron. Astrophys., 631, A96
Ivanov M. M., Simonović M., Zaldarriaga M., 2020a, JCAP, 05, 042
Ivanov M. M., Simonović M., Zaldarriaga M., 2020b, Phys. Rev. D, 101, 083504
Ivanov M. M., McDonough E., Hill J. C., Simonović M., Toomey M. W., Alexander S., Zaldarriaga M., 2020c, Phys. Rev. D, 102, 103502
James F., Roos M., 1975, Comput. Phys. Commun., 10, 343
Jiang J.-Q., Piao Y.-S., 2021, Phys. Rev. D, 104, 103524
Jiang J.-Q., Piao Y.-S., 2022, Phys. Rev. D, 105, 103514
Jiang J.-Q., Ye G., Piao Y.-S., 2022, preprint (arXiv:2210.06125)
Karwal T., Kamionkowski M., 2016, Phys. Rev. D, 94, 103523
Karwal T., Raveri M., Jain B., Khoury J., Trodden M., 2022, Phys. Rev. D, 105, 063535
Khosravi N., Farhang M., 2022, Phys. Rev. D, 105, 063505
Klypin A. et al., 2021, MNRAS, 504, 769
Knox L., Millea M., 2020, Phys. Rev. D, 101, 043533
Krishnan C., Colgáin E. O., Ruchika Sen A. A., Sheikh-Jabbari M. M., Yang T., 2020, Phys. Rev. D, 102, 103525
Lattanzi M., Gerbino M., 2018, Front. Phys., 5, 70
La Posta A., Louis T., Garrido X., Hill J. C., 2022, Phys. Rev. D, 105, 083519
Lemos P., Lee E., Efstathiou G., Gratton S., 2019, MNRAS, 483, 4803
Lesgourgues J., Pastor S., 2006, Phys. Rep., 429, 307
Lin M.-X., Benevento G., Hu W., Raveri M., 2019, Phys. Rev. D, 100, 063542
Mörtsell E., Dhawan S., 2018, JCAP, 09, 025
Mortsell E., Goobar A., Johansson J., Dhawan S., 2022, Astrophys. J., 933, 212
Murgia R., Abellán G. F., Poulin V., 2021, Phys. Rev. D, 103, 063502
Niedermann F., Sloth M. S., 2021, Phys. Rev. D, 103, L041303
Niedermann F., Sloth M. S., 2022, Phys. Rev. D, 105, 063509
Nojiri S., Odintsov S. D., Saez-Chillon Gomez D., Sharov G. S., 2021, Phys. Dark Univ., 32, 100837
Nunes R. C., Vagnozzi S., 2021, MNRAS, 505, 5427
Nunes R. C., Vagnozzi S., Kumar S., Di Valentino E., Mena O., 2022, Phys. Rev. D, 105, 123506
Oikonomou V. K., 2021, Phys. Rev. D, 103, 044036
Perivolaropoulos L., Skara F., 2022, New Astron. Rev., 95, 101659
Philcox O. H. E., Ivanov M. M., Simonović M., Zaldarriaga M., 2020, JCAP, 05, 032
Poulin V., Smith T. L., Karwal T., Kamionkowski M., 2019, Phys. Rev. Lett., 122, 221301
Poulin V., Smith T. L., Bartlett A., 2021, Phys. Rev. D, 104, 123550
Riess A. G. et al., 2022, Astrophys. J. Lett., 934, L7

Roy Choudhury S., Hannestad S., 2020, JCAP, 07, 037
Sabla V. I., Caldwell R. R., 2022, Phys. Rev. D, 106, 063526
Sakr Z., 2022, Universe, 8, 284
Sakr Z., Ilic S., Blanchard A., 2022, Astron. Astrophys., 666, A34
Sakstein J., Trodden M., 2020, Phys. Rev. Lett., 124, 161301
Schöneberg N., Franco Abellán G., Pérez Sánchez A., Witte S. J., Poulin V., Lesgourgues J., 2022, Phys. Rep., 984, 1
Smith T. L., Poulin V., Amin M. A., 2020, Phys. Rev. D, 101, 063523
Smith T. L., Poulin V., Bernal J. L., Boddy K. K., Kamionkowski M., Murgia R., 2021, Phys. Rev. D, 103, 123542
Smith T. L., Lucca M., Poulin V., Abellan G. F., Balkenhol L., Benabed K., Galli S., Murgia R., 2022, Phys. Rev. D, 106, 043526
Tanseri I., Hagstotz S., Vagnozzi S., Giusarma E., Freese K., 2022, JHEAp, 36, 1
Vagnozzi S., 2019, preprint (arXiv:1907.08010)
Vagnozzi S., 2020, Phys. Rev. D, 102, 023518
Vagnozzi S., 2021, Phys. Rev. D, 104, 063524
Vagnozzi S., Giusarma E., Mena O., Freese K., Gerbino M., Ho S., Lattanzi M., 2017, Phys. Rev. D, 96, 123503
Vagnozzi S., Dhawan S., Gerbino M., Freese K., Goobar A., Mena O., 2018, Phys. Rev. D, 98, 083501
Ye G., Piao Y.-S., 2020, Phys. Rev. D, 101, 083507
Ye G., Zhang J., Piao Y.-S., 2021, preprint (arXiv:2107.13391)
Ye G., Jiang J.-Q., Piao Y.-S., 2022, Phys. Rev. D, 106, 103528
Zumalacarregui M., 2020, Phys. Rev. D, 102, 023523

APPENDIX A: FREQUENTIST TABLE

We present the full table of frequentist results considering the combination of *Planck* and BOSS data. Some of this information is displayed graphically in Figs. 3 and 4.The full set of frequentist results showing the breakdown of the χ^2 and parameter shifts is shown in Table A1. The baseline results for this work were produced following the minimization routine of Schöneberg et al. (2022). We checked that MIGRAD recovers a similar trend, albeit with χ^2 values consistently higher than S21.

APPENDIX B: DATA COMPARISONS

We checked how different combinations of BOSS data affect the results presented in this analysis. Fig. B1 shows corner plots for different combinations of the datasets we used. There is a clear gain in the constraining power of the data on M_ν when moving from *Planck* alone (blue) to any of the contours that contain BOSS data in addition. However, there is little difference between the *Planck* + *BAO* and *Planck* + *BAO* + *FS* constraints, confirming earlier results in the literature (Ivanov, Simonović & Zaldarriaga 2020b). The most stringent constraint on M_ν is obtained when in addition to *Planck* data we consider the post-reconstruction BAO likelihood ($M_\nu < 0.144$ eV), which suggests that geometric features in BOSS data are what drive the constraints in the full FS + BAO likelihood for which we find $M_\nu < 0.151$ eV (on the other hand from the *Planck* + FS combination, we find the looser constraint $M_\nu < 0.210$ eV). These results all agree with earlier findings in the literature (see e.g. Ivanov et al. 2020b; Tanseri et al. 2022), confirming that the constraining power for M_ν of BOSS data is mostly contained in the geometrical, rather than shape information. This explains the marginal role the amplitude of clustering (as opposed to the position of the BAO peaks) appears to play in our M_ν constraints, as discussed throughout the paper. Finally, it is worth pointing out that the FS and combined FS + BAO likelihoods feature seven additional EFTofLSS nuisance parameters compared to the BAO-only likelihood.

Table A1. *Upper half* breakdown of the best-fitting χ^2 contributions from each likelihood and the total best-fitting χ^2, within different models ('EDE$_x$' indicates an EDE model with fixed $M_\nu = x$ eV). *Lower half* best-fitting values of H_0, σ_8, Ω_m, S_8, ω_c, and $f_{\rm EDE}$ within each model.

	Individual best-fitting χ^2 contributions							
Likelihood/model	ΛCDM$_{0.06}$	EDE$_{0.06}$	EDE$_{0.09}$	EDE$_{0.12}$	EDE$_{0.15}$	EDE$_{0.18}$	EDE$_{0.24}$	EDE$_{0.3}$
BOSS (BAO + FS)	297.2	295.3	295.4	295.5	295.9	296.5	298.2	301.9
Planck TTTEEE	2345.5	2342.6	2343.2	2343.7	2345.1	2345.5	2347.2	2348.3
Planck lowE	396.3	396.1	396.4	396.8	396.5	397.0	397.3	397.7
Planck lowl	23.2	21.9	21.7	21.5	21.3	21.2	21.1	21.1
Planck lensing	8.8	9.47	9.34	9.18	9.15	9.07	9.01	9.07
Total χ^2 (S21)	3071.0	3065.4	3065.9	3066.7	3067.9	3069.3	3072.9	3078.1
(MIGRAD)	3078.6	3070.7	3072.7	3073.0	3073.4	3076.0	3076.5	3088.3
	Best-fitting parameters							
H_0 [km/s/Mpc]	67.59	70.08	69.96	69.97	70.12	70.12	70.11	69.42
σ_8	0.811	0.828	0.824	0.820	0.814	0.811	0.802	0.787
Ω_m	0.312	0.306	0.309	0.311	0.312	0.315	0.319	0.325
S_8	0.827	0.837	0.836	0.834	0.831	0.831	0.826	0.819
ω_c	0.120	0.127	0.128	0.128	0.129	0.130	0.131	0.130
$f_{\rm EDE}$	–	0.077	0.082	0.089	0.099	0.107	0.117	0.117

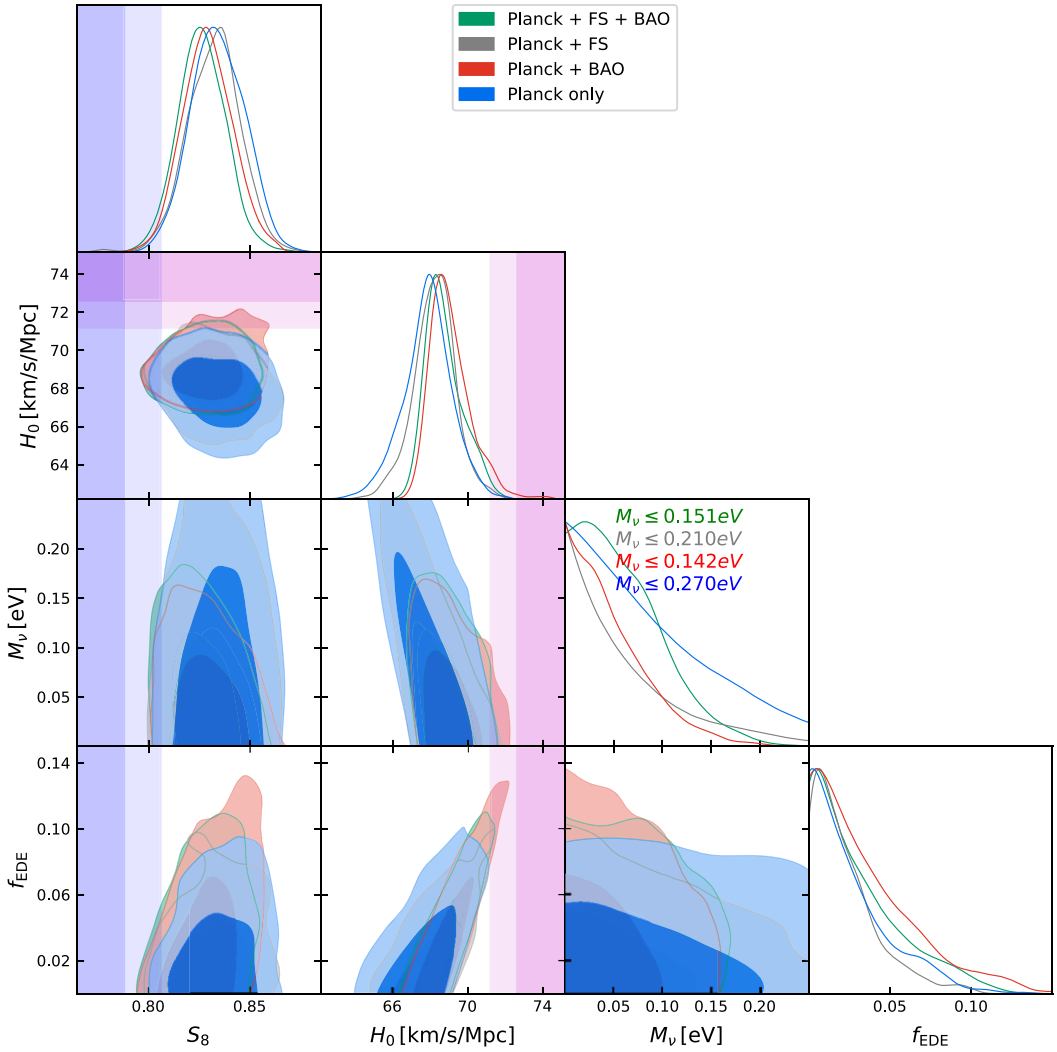

Figure B1. MCMC contours for the EDE + M_ν model obtained from several combinations of BOSS (FS and/or BAO) and *Planck* data.

This paper has been typeset from a TEX/LATEX file prepared by the author.